

PROBA-3 Precise Orbit Determination based on GNSS observations

Werner Enderle, *Prof. Dr.-Ing., Navigation Support Office, ESOC at ESA*

Francesco Gini, *Dr.-Ing., Navigation Support Office, ESOC at ESA*

Erik Schönemann, *Dr.-Ing., Navigation Support Office, ESOC at ESA*

Volker Mayer, *Ing., Navigation Support Office, ESOC at ESA*

BIOGRAPHY (IES)

Werner Enderle is the Head of the Navigation Support Office at ESA's European Space Operations Center (ESOC) in Darmstadt, Germany. Previously, he worked at the European GNSS Authority (GSA) as the Head of System Evolutions for Galileo and EGNOS and he also worked for the European Commission in the Galileo Unit. For over 20 years, he has worked on activities related to the use of GPS/GNSS for space applications. He holds a master and doctoral degree in aerospace engineering from the Technical University of Berlin, Germany.

Francesco Gini is a Navigation Engineer at the Navigation Support Office at the European Space Operations Centre (ESOC) of ESA. He is responsible for the Space Service Volume (SSV) and Precise Orbit Determination (POD) related activities. He received his PhD in Astronautics and Satellite Sciences at the University of Padova in 2014 and since then he has been working in ESOC.

Erik Schoenemann has joined the Navigation Support Office at ESA/ESOC in 2006 as a contractor and became permanent staff in 2015. He is involved in Galileo studies since the launch of the first Galileo validation satellite GIOVE-A and is the technical manager of the Galileo Reference Service Provider (GRSP). He is involved in the coordination of ESA's reference frame activities and contribution to International Services like ILRS, IGS and UTC. Erik Schoenemann holds a master and a doctoral degree in Geodesy from the Technical University of Darmstadt, Germany.

Volker Mayer is a member of the ESA/ESOC Navigation Support Office since 2015. He develops and operates ESA's Multi-GNSS high-precision orbit and clock product generation routines, for projects such as the ESOC MGNSS Finals, the GRSP Processing Facility 2 and Copernicus POD. With his expertise on Galileo signal processing and POD, he supports various navigation projects to meet their individual requirements. He graduated from the University of Stuttgart with a Master's degree in Geodesy and Geoinformatics in 2015.

ABSTRACT

ESA's PROBA-3 mission will demonstrate high-precision formation-flying of a pair of satellites in a High Eccentric Orbit (HEO) with new developed in-orbit technologies. It is a solar coronagraph science experiment consisting of two spacecraft, where the telescope of the solar coronagraph is mounted on one spacecraft, while the other spacecraft is maneuvered to block the solar disk as seen from the coronagraph spacecraft. The launch of the spacecraft is expected in late 2020. The PROBA-3 spacecraft pair will fly divided between periods of accurate formation flying, when payload observations will be possible, and periods of free flight. Each spacecraft will be able to maneuver itself. The typical separation distance between the two spacecraft will be about 200 m and 2 km, depending on the orbital phase. For the simulations, a separation distance of 200 m has been used. As the second spacecraft carrying the occultation disk is maneuvered relative to the primary spacecraft with the coronagraph on-board both spacecraft are considered to fly in the same orbit.

ESA's Navigation Support Office, located at the European Space Operations Centre in Darmstadt, Germany will use this ESA mission to test, analyze and demonstrate advanced concepts for spacecraft Precise Orbit Determination. This paper will provide an overview of the expected performance for absolute- and relative satellite POD for the PROBA-3 mission, based on simulations conducted in the preparation for this mission.



Figure 1: Principle of PROBA-3 solar coronagraph science experiment

INTRODUCTION

Each of the two PROBA-3 spacecraft will have a GNSS receiver on-board with the capability of tracking multi-frequency (dual freq.), multi-signal and also multi GNSS constellation (Galileo and GPS). In addition, the GNSS equipment consists also of two antennas on each satellite, a high gain antenna, which will point towards the Earth during the Apogee phase of flight and a patch antenna, pointing away from the Earth, which will be used during the perigee phase of the flight. PROBA-3 will fly below the altitude of the GNSS constellations during the perigee phase and above the altitude of the GNSS constellations during apogee phase. Considering the recent developments related to the interoperable GNSS Space Service Volume (SSV), which is supported by all GNSS providers, the PROBA-3 mission can be considered as an ideal case to demonstrate the benefits of an interoperable GNSS SSV on end-user level.

With a perigee altitude of about 600 km and an apogee altitude of about 60,530 km PROBA-3 provides a perfect test platform to demonstrate the availability of GNSS signals in space, in terms of signal reception and signal strength, covering a very large altitude range, very different geometry conditions and also dynamics of the satellites in terms of velocity conditions.

In this paper, the analysis of the GNSS visibility conditions for PROBA-3 will be assessed via a link-budget approach and the visibility results will be presented. Based on this scenario, realistic GNSS observations will be simulated and later on processed with a Precise Orbit Determination (POD) approach. The results of the PROBA-3 POD will be then presented and discussed in terms of absolute and relative orbital accuracy.



Figure 2: Orbit configuration for PROBA-3 solar coronagraph science experiment geometry

GNSS SIGNAL AVAILABILITY ANALYSIS

The general situation related to the relative geometry between GNSS satellites and space user satellites is outlined in Figure 3. As can be seen, the geometrical visibility conditions are strongly depending on the orbit altitude and also on the possibility to use signals from the Main Lobe and the 1st Side Lobe in the Link-Budget calculations.

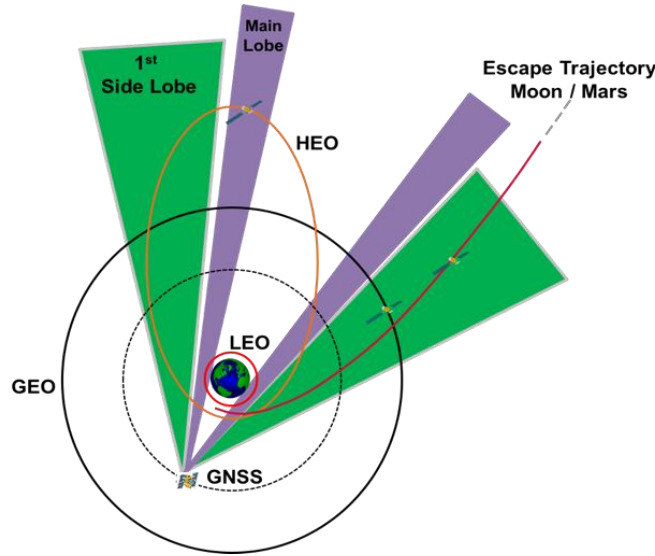


Figure 3: Relative geometry between GNSS constellations and space user for visibility analysis

GNSS signal availability simulations setup for PROBA-3

In order to accurately assess the expected GNSS signal availability in space for the PROBA-3 mission, it is important to have realistic assumptions and the associated simulation setup. The setup adopted for this study is hereafter described. The orbital elements for the PROBA-3 satellites are defined in Table 1.

Table 1. PROBA-3 satellites - orbital elements.

Osculating elements	PROBA-3 master / chaser
a	36943 km
e	0.8111
i	59 deg
ω	188 deg
Ω	152 deg
ϑ	0 deg / -0.016 deg
Altitude at perigee	601 km
Altitude at apogee	60529 km
Relative separation at perigee	2 km
Relative separation at perigee	0.2 km

As each PROBA-3 satellite will carry a dual-frequency multi-constellation (Galileo and GPS) receiver, the Galileo and GPS constellations in their actual configuration were used for this analysis. The actual constellations consist of a total of 24 satellites for Galileo deployed into 3 orbital planes and 31 for GPS deployed into 6 orbital planes.

In order to evaluate the GNSS signals availability, an accurate link-budget analysis has been carried out. This has the objective of evaluating the GNSS signals carrier-to-noise ratio CN0 received by PROBA-3 along its orbit, and to determine whether these signals can actually be acquired and tracked by the on-board receivers. For this reason, several parameters have to be defined and also several assumptions have to be made for the link-budget calculation. The parameters and assumptions are described in the following part.

For the GNSS Effective Isotropic Radiated Power (EIRP), the following models were adopted in our simulations:

- For the Galileo E1 and E5a EIRP models, ESOC’s Navigation Support Office derived conservative values for the side lobes from the ICG agreed values for the main lobe, as defined in the SSV Booklet [2]. This model is shown in Figure 4, left hand-side. In his context, it is important to understand that this model is not an official ESA model for the Galileo side lobes, it is just an ESA/ESOC internal assumption.
- Results from a NASA experiment were used, by which the antenna patterns of the various GPS blocks for L1 was measured from space, by means of a single frequency receiver on board a geostationary satellite. The GPS Antenna Characterization Experiment (GPS ACE) [3,4], for which the data are available online, were used to reconstruct the EIRP for the GPS L1 frequency and were used in this study for the GNSS signals availability analysis.
- In 2014 Lockheed Martin [5] published the legacy and improved GPS antenna patterns for the L1 and L2 for the different satellites. From these values, it has been possible to derive the expected improved EIRP and use the L2 values in our simulations. The GPS EIRP values adopted in the frame of this study are shown in Figure 4, right hand-side.

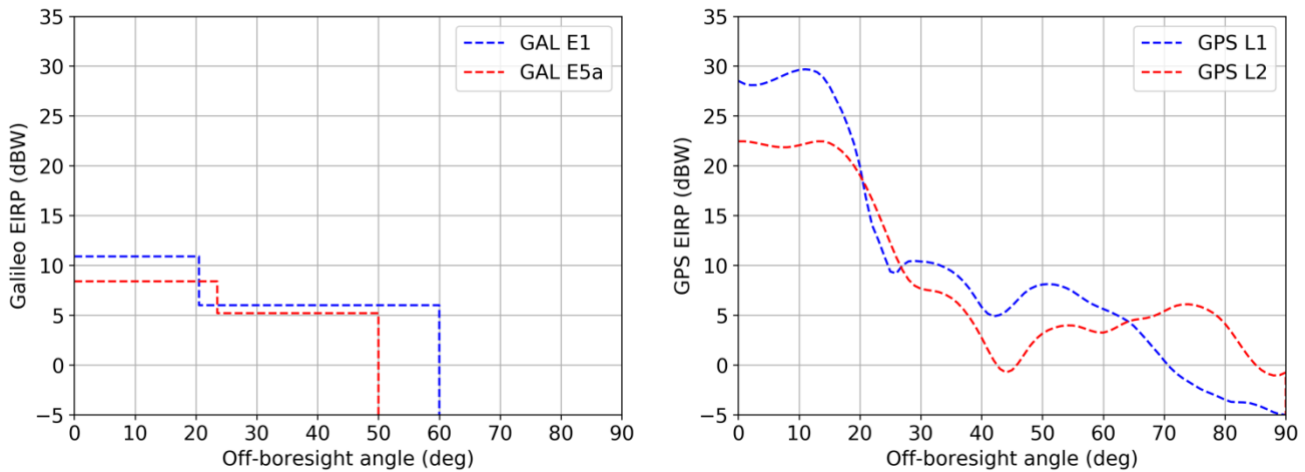


Figure 4: ESA/ESOC non-official Galileo E1 and E5a EIRP models on the right and GPS L1 (ACE) and L2 (Lockheed Martin) EIRP values on the left-hand side as a function of the off-boresight angle.

As can be observed in Figure 4, the Galileo values are very conservative compared to the GPS EIRP, which have higher value for the main lobe and have full extension of the side lobes up to 90 degrees of off-boresight angle.

The GPS ACE L1 EIRP (computed as the mean of all the values) shows a much higher primary lobe. Up to 30 dBW at the peak, and also shows that a significant amount of power is emitted in the off-boresight directions, with more than 0 dBW up to 70 angle degrees. A similar pattern is visible for the Lockheed Martin L2 EIRP, which shows a good consistency with the ACE L1 values. The main lobe for the Lockheed Martin pattern is about 23dBW, a bit lower than the ACE L1 values, but on the other hand it has higher secondary lobes, with EIRP values above the 0 dBW up to 90 degrees. The results shown later in this analysis, will show that the secondary lobes are extremely important for the SSV GNSS signals availability and therefore allowing receivers to track GNSS signals at extremely high altitudes, in particular above the GNSS MEO constellations. An important note on **Error! Reference source not found.**, regarding the ACE EIRP. NASA provides the antenna patterns in the off-boresight range 16-90 degrees. Below 16 degrees the signal is obstructed by the Earth. For completeness of the antenna patterns, the ACE gap has been filled with the GPS L1 Lockheed Martin pattern, scaled to match the boundary value at 16 deg. This is a simple assumption, not based on real measurement, that will not affect the results presented in this study. Because of the Earth blockage, this range of signal can only reach the LEO part of the PROBA-3 orbit, where the CN0 of the signals are in any case higher than the defined acquisition and tracking thresholds.

For what concerns the receiver’s link-budget parameters, the PROBA-3 satellites in our simulations have been equipped with two GNSS antennas. As the satellites attitude is nadir-pointing we have implemented a Low-Gain (LG) patch antenna pointing in the zenith direction and a high-gain antenna (HGA) pointing in the nadir direction. The antenna patterns are shown in Figure 5. This design was selected, because the highly-eccentric orbit has an altitude of 600 km at perigee (LEO) and 60000 km at apogee. Hence, the trajectory is partly below and partly above the Galileo and GPS altitude. In the LEO region, a standard GNSS receiving antenna is sufficient to allow the receiver to acquire and track the GNSS signals, as they will have a high CN0. On the other hand, as soon as PROBA-3 flies above the GNSS constellations towards the apogee the GNSS signals CN0 will drop significantly. Hence a high-end HGA with about 9 dBi gain in the boresight direction is needed to increase the CN0 as much as possible as in the apogee region the GNSS CN0 levels become extreme, as it will be shown in the next section.

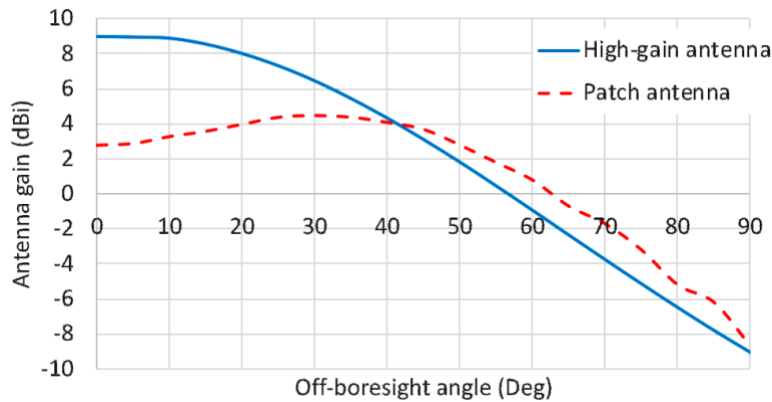


Figure 5: PROBA-3 receiver antenna patterns. Nadir-pointing patch antenna pattern and zenith-pointing high-gain antenna pattern.

Concerning the tracking and acquisition CN0 for the PROBA-3 receiver, the thresholds have been set up to 20 dBHz. For simplicity, the acquisition and tracking CN0 thresholds have been assumed to be equal. In conclusion, the signal availability analysis has been conducted for the following ERIP models summarized in Table 2.

Table 2. PROBA-3 simulated scenarios configuration.

Galileo EIRP	GPS EIRP
ESA/ESOC E1 model	ACE L1 model
ESA/ESOC E5a model	Lockheed Martin L2 model

The link-budget calculation approach, as described in the SSV Booklet has been adopted within this analysis.

GNSS signal availability results

This section contains the results for the simulated scenario. Figure 6 shows the GNSS signals availability for the 20dB-Hz receiver acquisition and tracking CN0 threshold, for a 24-hours arc, starting at the perigee of the PROBA-3 orbit. The visibility pattern that can be observed in all this figure shows a high number of GNSS satellites being tracked around the perigee by the zenith-pointing patch antenna (LG=Low-Gain), while the nadir pointing high-gain antenna (HG) provides a high signal availability when PROBA-3 reaches the altitude of the GNSS constellations and above them. The main factors that limit the GNSS availability around the apogee are: 1) the Earth occultation, which blocks the GNSS signals main lobe and 2) the limited power in the secondary lobe, which in most cases is not enough to guarantee coverage at high altitudes. It can be observed in this scenario that, thanks to the secondary lobe, both the Galileo and GPS constellations provide a sufficient number of available signals throughout all the orbit, even at the apogee located at an altitude of more than 60000 km. Figure 6 shows that with a more advanced receiver, capable of tracking weaker signals, it is possible to achieve full coverage for the PROBA-3 mission. It also demonstrates how conservative the ICG results shown in [2] are and the big improvement, in terms of available signals, that derive from the side lobes.

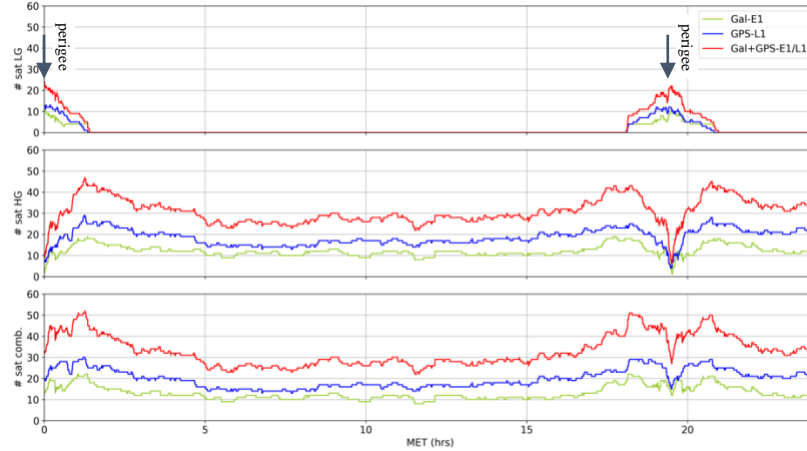


Figure 6: GNSS signal availability for a CN0 receiver threshold of 20dB-Hz for the Galileo E1 and GPS L1 frequencies.

Table 3 summarizes and compares the GNSS signals availability along the PROBA-3 orbit, for a CN0 threshold of 20dB-Hz, for the combined patch + high-gain antenna tracking. The higher signals availability for the GPS constellation is a direct consequence of the higher and wider EIRP model adopted in the simulations and of the larger constellation (31 satellites as compared to 24 for Galileo). It is possible to see that an interoperable receiver and processing which makes use of all the GNSS signals reaching PROBA-3 will allow the signal tracking along the entire PROBA-3 orbit, with a minimum of 23 visible signals available for POD. The results obtained in terms of signals availability are considered as outstanding. The results obtained for the E5a/L2 signals are in line with what has been shown here for the E1/L1 signals.

Table 3. Number of available GNSS signals along the orbit of PROBA-3 for the patch + high-gain antenna tracking for the E1/L1 frequencies.

	Galileo available signals	GPS available signals	Combined signals availability
Perigee	12	18	30
MEO altitude	21	28	49
Apogee	8-13	15 – 18	23 - 31

PRECISE ORBIT DETERMINATION ANALYSIS

Precise Orbit Determination setup and processing

Based on the GNSS signals availability described in the previous section, a Precise Orbit Determination (POD) campaign was set up. Galileo E1 and E5a and GPS L1 and L2 code and carrier-phase observations have been simulated for a reference orbit of PROBA-3, for the two satellites. The same orbits, attitude, signal structure and link-budget parameters have been chosen for the POD simulation as defined in the previous section.



Figure 7: GNSS signals simulation, POD processing and orbital accuracy analysis flowchart.

Figure 7 shows the three-steps approach used for the POD analysis. The first step is the generation of the GNSS observations, the second is to process them with a POD approach and the third and final step is the evaluation of the estimated orbits accuracy in terms of absolute and relative accuracy. Table 4 shows the main parameters setup adopted in the signal generation and processing. As can be observed, in the signal's simulations, the most accurate solutions and models have been used, while, on the processing side, less accurate solutions and noise have been introduced, in order to simulate a realistic scenario. In particular, with respect to the GNSS satellites orbits and clocks the ESA/ESOC MGNSS final solution with fixed carrier-phase ambiguities [6] have used in the simulation to generate the GNSS signals. When processing these signals the ESA/ESOC solutions with float ambiguities were used, in order to introduce realistic errors in the GNSS ephemerides and clocks. The 3D RMS in the orbital differences between the two adopted GNSS solutions is about 5 cm. With respect to the GNSS signals simulated, a realistic white noise and bias have been added to the observations as a function of the CN0 received by the PROBA-3 receivers. These observations have been then processed based on a single frequency linear combination (GRAPHIC linear combination), and based on a dual-frequency linear combination (ionospheric-free linear combination). With respect to the user orbit, in terms of dynamical models, a high degree and order gravity field (120x120) has been used in the simulation, while a lower degree and order gravity field (80x80) has been used in the simulations in order to introduce some error in the satellite dynamics. For the same reason an accurate box-wing model has been used in the simulation of the solar and Earth radiation pressure effects and the satellite aerodynamics, while a 10% error has been introduced to these models when processing the observations. When processing the observations, a set of empirical accelerations, Cycle-Per-Revolution (CPRs) in the along and cross-track direction, have been estimated in order to empirically absorb the dynamical perturbations. This is the approach commonly used when processing real data from space receivers, in order to absorb the residual perturbations that were not perfectly caught by the models. No CPRs have been used when simulating the GNSS signals.

Table 4. Observations generation and processing setup.

Parameter category	Parameter	Simulation setup	Processing setup
GNSS Satellites	GNSS satellite orbits and clocks	ESA/ESOC final solution with fixed ambiguities	ESA/ESOC final solution with float ambiguities
GNSS Observations	Code + Phase	E1 & E5a, L1 & L2 with noise + bias $f(\text{CN0})$	Linear combinations SF: GRAPHIC E1/L1 DF: iono-free
User Orbits	Gravity field	120x120	80x80
	Radiation pressure and aerodynamics	Box-wing model	Box-wing model with 10% error
	Empirical accelerations	-	1 set CPR in along- and cross-track

The duration of the simulation is one PROBA-3 orbital period (19.6 hours) starting and ending at the perigee, with GNSS observations sampled every 10 seconds.

The simulated GNSS observations have been processed using the dynamic Least-Square-Adjustment approach. The initial state vector and 3 empirical piecewise constant parameters in the along- and cross-track directions have been estimated in order to absorb the dynamical perturbations. Additionally, the receivers' clocks and carrier phase ambiguities have been estimated respectively epoch-wise and pass-wise.

Different approaches can be selected to treat the observations. If more than one frequency is available, the signals could be combined in an ionospheric-free linear combination. Even though this is the most frequently chosen approach, it has the limitation that when either one signal is not available the linear combination cannot be formed and hence useful observations are discarded. In addition, at high altitudes such as the SSV zone, no atmospheric effects are present and the linear combination is not useful. In terms of observations, three approaches have been identified. The observations can be processed using:

1. the GRAPHIC linear combination, which is the single frequency ionospheric free linear combination of code and phase measurements on the same carrier, which eliminates the ionospheric delays and keeps the observations on different carriers

independent. As shown in Equation 2 and 3 the noise of this observation is very high, as it is very close to half the noise of the code observations noise, in the order of 0.5 m.

2. the ionospheric-free linear combination, which is a dual frequency linear combination which also eliminates the ionospheric delays. This can be formed between the carrier phase observations on two frequencies and/or between the code observations on two frequencies. As shown in Equation 4 and 5 the noise of this observation for the phase observations is a bit higher than the carrier phase observations noise, but still in the order of 1 cm.
3. the RAW approach, where no linear combinations or differentiation of signals is applied. This approach maintains the noise in the observations to a pure minimum. However, in the context of the simulations for this paper, the RAW approach has not been implemented. More information about the RAW approach can be found in [7].

The tropospheric delays can be ignored for PROBA-3 as the GNSS signals received by the pair of satellites is not passing through the troposphere, and also other effects such as multipath or relativistic effects were ignored. The single frequency GRoup And Phase Ionospheric Correction (GRAPHIC) linear combination can be derived as:

$$GRAPHIC_r^s = \rho_r^s + c[dt_r - dt^s] + \frac{\lambda_i N_{r,i}^s}{2} + \frac{\epsilon_P + \epsilon_L}{2} \quad (1)$$

where:

- r and s are respectively referred to the receiver and the GNSS satellite
- c is the speed of light
- dt are the clock biases for the receivers and transmitters
- T is the tropospheric delay
- I is the ionospheric delay
- λ is the wavelength of the GNSS wave
- N in the carrier-phase integer ambiguity

ϵ is the pseudorange and carrier-phase measurement noise.

As can be observed in Equation 1, the GRAPHIC observation type contains the ambiguity term from the phase observation and, as observation noise, has the average between the code and phase observations noise. In general, being the code noise much higher than the phase noise the noise on the GRAPHIC observations is

$$GRAPHIC\ noise = \frac{\epsilon_P + \epsilon_L}{2} \sim \frac{\epsilon_P}{2} \quad (2)$$

about half the noise of the code observations. In general, the noise on the code observations is in order of several decimeters while for the phase observations the noise is at the millimeter level.

For what concerns the dual-frequency (frequencies i and j) ionospheric free linear combination, this can be derived for the carrier phase as:

$$ionofree_r^s(i, j) = \rho_r^s + c[dt_r - dt^s] + \frac{f_i^2 \lambda_i N_{r,i}^s - f_j^2 \lambda_j N_{r,j}^s}{f_i^2 - f_j^2} + \epsilon_{ionofree} \quad (3)$$

where the noise term, based [8], is about 3 times higher than the phase noise for the L1-L2 linear combination, and about 2.6 times higher than the phase noise for the E1-E5a linear combination.

Having assumed in our simulations a noise level for the code observations of 70 cm (1sigma) and for the phase observations of 7 mm (1sigma), it can be easily derived that in our simulations the noise levels for the three described approaches are the following:

1. the GRAPHIC linear combination has a noise of 35 cm;
2. the ionospheric-free linear combination between carrier-phase observations has a noise of about 1.8 cm for the Galileo E1-E5a and about 2cm for the GPS L1-L2 linear combinations;
3. the RAW approach will maintain the original levels of noise unchanged.

The RAW approach is for several reasons considered as the optimal solution by ESOC's Navigation Support Office. One of the benefits of the RAW approach is that it works with observations on a single or on two frequencies, whereas the IonoFree method is only working if both L1 and L2/E5 is available. However, the RAW approach needs a deeper and more detailed analysis, carefully treating the observation biases, and it will not be treated in this paper, but it will be addressed in a future dedicated study. Hence, the

POD results in this paper will be presented and discussed based on the first two options, namely the single frequency GRAPHIC linear combination for Galileo E1 and GPS L1 (common frequency among all systems) and the ionospheric-free linear combination Galileo E1-E5a and GPS L1-L2.

Precise Orbit Determination results

The results of the POD processing of the PROBA-3 Galileo + GPS observations are presented here in terms of absolute and relative orbital accuracy. Figure 8 shows the absolute orbital difference between the POD orbit solution based on the GRAPHIC linear combination and the reference orbit, a-priori known and used to generate the observations. Figure 8 shows the absolute orbital difference for one of the PROBA-3 satellites (the other one is performing similarly) as a function of the Mission Elapsed Time (MET), which corresponds to the time along the orbit. On the left- and right-hand sides of the picture the satellite is at its perigee, in the central part it is at the apogee. It can be observed that the major component of the error is around the apogee area in the radial direction, with the error up to 40cm. This is most probably caused by the bad relative geometry of the PROBA-3 satellites and the GNSS constellations, leading to a bad Dilution Of Precision (DOP) and because the observations have been altered introducing noise and bias to simulate a more realistic scenario. The RMS of the absolute orbital error in the radial, along- and cross-track directions is respectively about 25.8 cm, 8.9 cm, and 9.1cm, accounting for a total 3D RMS of about 28.8 cm.

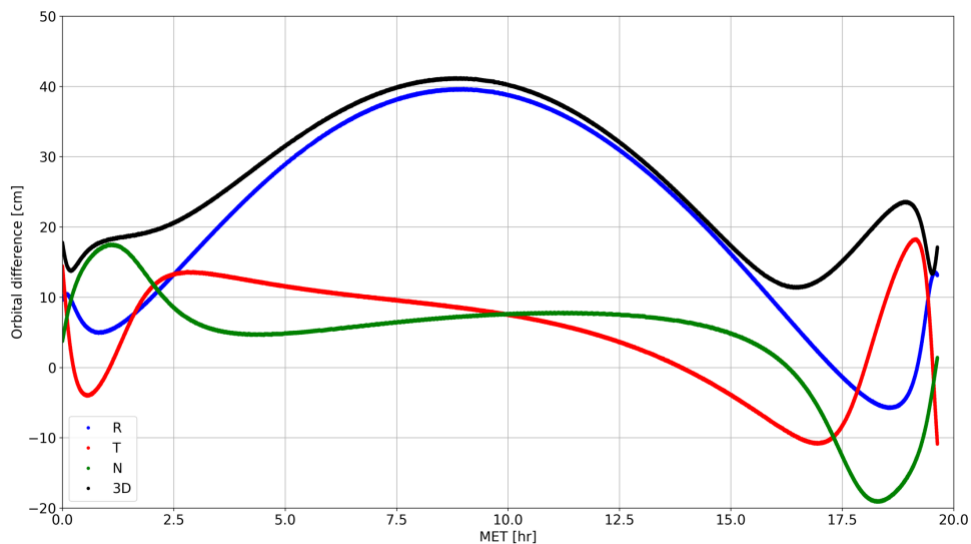


Figure 8: POD absolute orbital difference RMS for the single frequency GRAPHIC linear combination scenarios for a CN0 threshold of 20 dB-Hz.

Figure 9 shows the relative orbital difference between the POD orbit solutions based on the GRAPHIC linear combination and the reference orbits. The relative solution has been computed by subtracting epoch-wise the independently estimated absolute positions of the PROBA-3 satellites. This relative solution has been then compared to the reference relative solution. It can be observed that the major component of the error is again in the radial, up to about 20 cm. In terms of error components, the RMS in the radial direction is about 13.4 cm, in the along-track and cross-track it is about 1cm, for a total 3D RMS of about 13.5 cm.

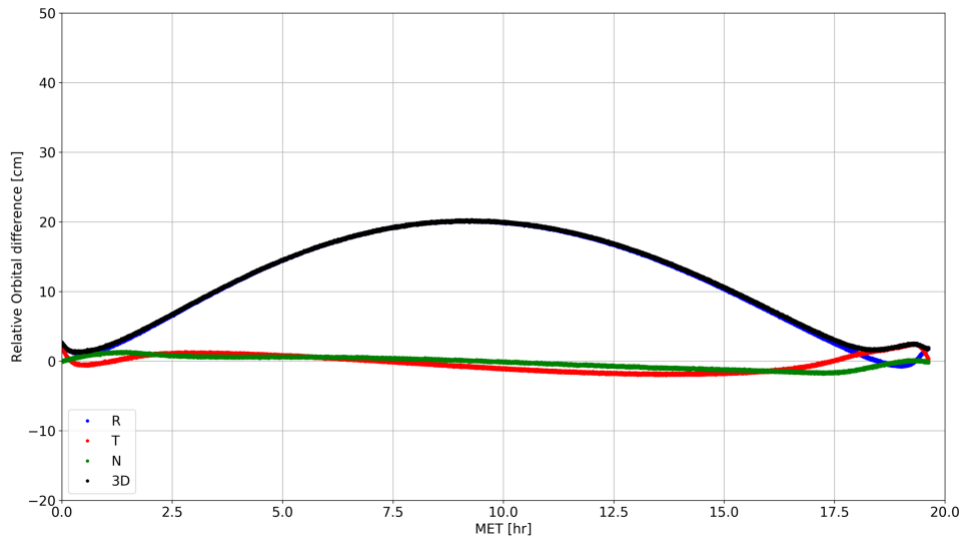


Figure 9: POD relative orbital difference RMS for the single frequency GRAPHIC linear combination scenarios for a CN0 threshold of 20 dB-Hz.

Figure 10 shows the absolute orbital difference between the POD orbit solution based on the dual-frequency ionospheric-free linear combination. As said earlier, the noise of the iono-free phase observations is much lower than the GRAPHIC's, and this is also visible in the results. The absolute orbital error is again showing its maximum error at the apogee, with about 13.1 cm in the radial direction, which is on the other hand about half of the GRAPHIC's absolute error. The RMS in the along-track is about 3cm and it is 5 cm in the cross-track direction, for a total of 14.3 cm 3D.

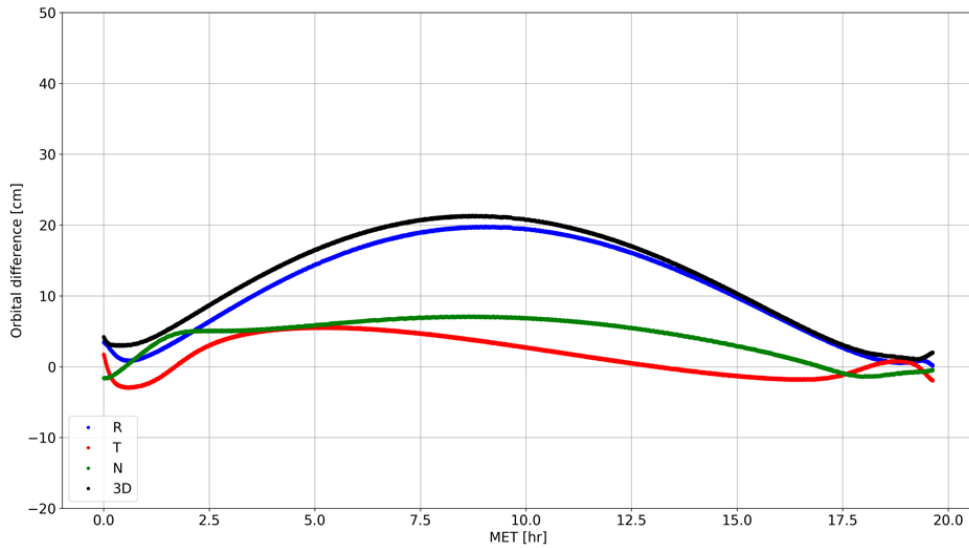


Figure 10: POD absolute orbital difference RMS for the dual frequency ionospheric-free linear combination scenarios for a CN0 threshold of 20 dB-Hz.

Figure 11 shows the relative orbital difference between the POD orbit solutions based on the dual-frequency ionospheric-free linear combination and the reference orbits. It has to be noted that the scale in this plot is different from the previous ones. This is because the accuracy achieved with this scenario is much better. The relative orbital error is now equally spread over the 3 components where each component has at most 2 mm RMS and the total 3D RMS is about 3 mm. This is an outstanding result which clearly demonstrates the improvement in the POD approach deriving from the less noisy observations. In particular, in a scenario where at the apogee the

PROBA-3-GNSS satellites relative geometry is bad and the GNSS DOP is very high, the availability of signals with the lowest noise is the best option, as it leads to most accurate solutions in terms of both absolute and relative positioning.

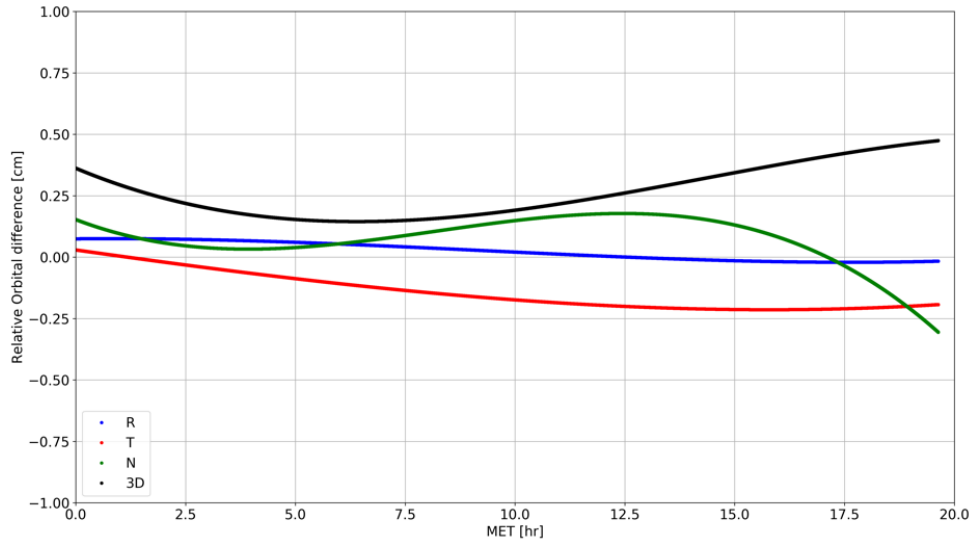


Figure 11: POD relative orbital difference RMS for the dual frequency ionospheric-free linear combination scenarios for a CN0 threshold of 20 dB-Hz.

CONCLUSION

Concerning the GNSS Signal Availability analysis for PROBA-3, it has been confirmed that the results from ICG are very conservative, because only the main lobe is considered. Taking into account the GPS L1 ACE estimated antenna pattern (main lobe + side lobe), which is considered as being consistent with the data sheets from Lockheed Martin and taking also an assumed conservative antenna pattern for Galileo (main + side lobe) – ESOC assumption, no ESA official – into account, one will obtain a significant improved GNSS signal availability for PROBA-3 compared to ICG. As a consequence, a GNSS receiver capable of acquiring and tracking a signal level of 20 dB-Hz CN0 will have GNSS signal availability of more than 4 GNSS satellites for the entire PROBA-3 orbit.

Precise Orbit Determination based on single frequency GRAPHIC observations provided results for absolute orbit error, 3D RMS of about 29 cm with the largest contribution from the radial error. The relative orbit error, based on the processing of the GRAPHIC observations was about 14 cm, 3D RMS.

Precise Orbit Determination based on the processing of dual-frequency ionospheric-free linear combination of Galileo and GPS observations provided an absolute orbit error of 14.3 cm 3D RMS, with the largest contribution in radial direction. The relative orbit error for the processing of dual-frequency ionospheric-free linear combination of Galileo and GPS observations is in the order of 3mm, 3D RMS.

The obtained results showing clearly the advantages for the processing of dual-frequency ionospheric-free linear combination of Galileo and GPS observations compared to the processing of the GRAPHIC observations. The orbit accuracy could be improved by a factor of 2 for the absolute POD and even by around 2 orders of magnitude for the relative POD. However, ESOC’s Navigation Support Office believes that the RAW approach will provide even better results for PROBA-3 absolute and also relative POD.

ACKNOWLEDGMENTS

Sincere thanks to our ESA/ESTEC colleagues from the PROBA-3 project team for an open, fruitful and productive cooperation.

REFERENCES

1. https://www.esa.int/Our_Activities/Space_Engineering_Technology/Proba_Missions/Mission2
2. *The Interoperable Global Navigation Satellite Systems Space Service Volume*, United Nations, Vienna 2018
3. <https://esc.gsfc.nasa.gov/navigation>
4. J.E. Donaldson et al., “Characterization of On-Orbit GPS Transmit Antenna Patterns for Space Users”, Feb 2019
5. Marquis, *GPS Block IIR and IIR-M Antenna Panel Pattern*, Feb 2014
6. ESA/ESOC GNSS solutions: http://navigation-office.esa.int/GNSS_based_products.html
7. Reckeweg F., Schönemann E., Springer T., Becker M., Enderle W., “Multi-GNSS / Multi-Signal code bias determination from RAW GNSS observations”, *Proceedings of the Geodätische Woche (InterGEO 2016)*, Hamburg, Germany, October 2016
8. DOPS-SYS-TN-0100-OPS-GN, “NAPEOS Mathematical Models and Algorithms”, ESA/ESOC, November 2009